COBEM 2021 26th International Congress of Mechanical Engineering
November 22-26, 2021, Virtual Congress, Brazil

COB-2021-0751
FEASIBILITY OF OPTICAL PROFILOMETRY FOR QUALITY CHARACTERIZATION OF MONOLAYER PARTS OBTAINED BY FUSED FILAMENT FABRICATION

Thiago Glissoi Lopes
Matheus Godoy Fonseca do Carmo
São Paulo State University, Av. Eng Edmundo C. Coube, 14-01 - Núcleo Hab. Pres. Geisel, Bauru – SP, 17033-360
thiago.glissoi@unesp.br, matheusgodyfcarmo@gmail.com

Laura Marques Queiroz
Industrial Technical College "Prof. Isaac Portal Roldán", Av. Nações Unidas, 58-50 - Nucleo Res. Pres. Geisel, Bauru - SP, 17033-260
laura.marques@unesp.br

Paulo Roberto de Aguiar
São Paulo State University, Av. Eng Edmundo C. Coube, 14-01 - Núcleo Hab. Pres. Geisel, Bauru – SP, 17033-360
paulo.aguiar@unesp.br

Thiago Valle França
São Paulo State University, Av. Eng Edmundo C. Coube, 14-01 - Núcleo Hab. Pres. Geisel, Bauru – SP, 17033-360
thiago.franca@unesp.br

Abstract. *The growth in adoption of additive manufacturing processes, such as the Fused Filament Fabrication (FFF) process, as alternative to traditional subtractive manufacturing processes, has been perceived for industrial and end-consumer applications. The FFF process, also known as 3D printing, deals with the fabrication of parts by adding subsequent layers of fused plastic filaments. The manufacture of the first layer in the FFF process is considered to be critical, due to the fact that the first layer provides support for the upcoming ones. Thus, if a defect is detected in the fabrication of the first layer, the FFF process can be interrupted. This practice may result in the prevention of several losses due to an incorrect printed part. It is a common practice in FFF monitoring studies to print what is called a monolayer part. A monolayer part is usually a fabrication of a part consisting of a single layer, but it can also be determined to be the fabrication of just the first layer of a multilayered part. Optical profilometry is a well-known method of inspecting the surface quality of parts obtained by different manufacturing processes. Thus, the present work sought to study the feasibility of evaluating the surface quality of monolayer parts obtained by the FFF process by means of optical profilometry for failure detection purposes. The obtained results showed the feasibility of using optical profilometry to inspect the surface quality of monolayer parts obtained by the FFF process for failure detection purposes.*

Keywords: *3D Printing, Fused Filament Fabrication, Optical Profilometry, Part Evaluation, Failure Detection*

1. INTRODUCTION

The growth in adoption of additive manufacturing (AM) processes, such as the Fused Filament Fabrication (FFF) process, as alternative to traditional subtractive manufacturing processes, has been perceived for industrial and end-consumer applications (DHINAKARAN *et al.*, 2020; YEH; CHEN, 2018). One of the reasons that could explain the growth in adoption of AM process as alternative to traditional subtractive manufacturing processes is that a fabrication by means of AM processes can be completed in a short time, and that high dimensional accuracy can be achieved by adjusting the process parameters (DHINAKARAN *et al.*, 2020).

The FFF process, also known as 3D printing, deals with the fabrication of parts by adding subsequent layers of fused plastic filaments (LIU *et al.*, 2019). To fabricate a part by means of AM processes, such as the FFF process, one needs first to obtain a digital 3D model of the desired part (VOLPATO, 2017). The digital 3D model of the part can be obtained by means of computer aided design (CAD) software (ZWIER; WITS, 2016), for novel geometries, or digitization techniques (XU; DING; LOVE, 2017), for existent physical models. After the digital 3D model of the part has been obtained, the next step is to slice the digital model with the aid of a slicer software (KOCISKO *et al.*, 2017). In order to obtain a geometrically and overall surface desired printed part, the process operator needs to correctly establish the process parameters in the chosen slicer software (CARMO *et al.*, 2020). The final step in the procedure of fabricating a part by means of FFF process is to transmit the digitized data of the sliced part, written in G-Code, to the printer, in order to allow for the manufacture of the layers to start (KOCISKO *et al.*, 2017).

The manufacture of the first layer in the FFF process is considered to be critical, due to the fact that the first layer provides support for the upcoming ones (WU; YU; WANG, 2016). Thus, if a defect is detected in the fabrication of the first layer, by means of direct or indirect monitoring methods, the FFF process can be interrupted (CARMO *et al.*, 2020). The practice of monitoring the fabrication of the first layer may result in the prevention of several losses due to an incorrect printed part (WENDT *et al.*, 2016).

It is a common practice in FFF monitoring studies to print what is called a monolayer part (CARMO *et al.*, 2020). The monolayer part is usually a fabrication of parts consisting of just a single layer (CARMO *et al.*, 2020), but it can also be determined to be the fabrication of just the first layer of a multilayered part (LOPES *et al.*, 2020). The practice of printing a monolayer part is conducted in order to allow for evaluation of the overall correctness of the adopted process parameters, as reflected on the geometrical and mechanical attributes of the obtained part (CARMO *et al.*, 2020; WENDT *et al.*, 2016).

2. OPTICAL PROFILOMETRY

Surface quality is an important characteristic for many parts, as it can impact the part performance in a variety of areas such as light reflexivity, bio contamination potential, capacity to retain liquids (e.g. lubricant) and friction with adjacent surfaces. Surface roughness is a common parameter used when studying the surface quality and it is often a production requirement that a part's surface roughness stay within a certain range in order to assure the part/system correct functioning (ZHANG *et al.*, 2020).

A specimen's surface quality can be quantified using a profilometer to map the surface's profile (LUO *et al.*, 2020). This can be done either by a contact profilometer or by a non-contact profilometer. Optical profilometry is a non-contact type of profilometry where light is used to perform the profile assessment. This is done by assessing how the light is reflected by the surface's features and then analyzing its behavior (BLUNT, 2006). As examples of perceivable features, one may look into the difference in luminous intensity between emission and reflection or the location of interference fringes on different height positions can be used depending on the method employed (BLUNT, 2006; LEKSYCKI; KRÓLCZYK, 2021). The advantages of the optical approach include its scanning speed, generation of 2D and 3D topography images and no risk of damaging or contaminating the part (since contact is not required (ADI *et al.*, 2008; BLUNT, 2006)), as well as the capability of detecting irregularities that contact profilometry can't (NIESLONY *et al.*, 2017).

This measurement technique can be used in a wide range of applications and studies, for instance surface morphology of micron-sized particles used as drug ingredients and excipients (ADI *et al.*, 2008), porosity analysis of PEEK medical implants produced via AM in regards to osteoconductive (SPECE *et al.*, 2020), investigation of roughness and morphology of polishing different types of resin for dental restoration (GANTZ *et al.*, 2021), surface characteristics of rocks used as substrate by Benthic algae, used on water remediation (KHOSHKHOO *et al.*, 2017), among others. In more tech-focused fields it has been used: as a feasible way for inspecting the surface of semiconductor waffles under production conditions (BLUNT, 2006), comparing results of chemical and electropolishing of internal surfaces (TYAGI *et al.*, 2019); Porosity characterization of micro grinding tools (SETTI; KIRSCH; AURICH, 2019), among others.

In the context of optical profilometry, the authors have not found in literature papers that present studies regarding the evaluation of the surface quality of FFF printed monolayer parts. Thus, the present work sought to study the feasibility of evaluating the surface quality of monolayer parts obtained by Fused Filament Fabrication process by means of optical profilometry for failure detection purposes.

3. MATERIAL AND METHODS

3.1 Printing setup

In order to study the feasibility of evaluating the surface quality of monolayer parts obtained by Fused Filament Fabrication process by means of optical profilometry for failure detection purposes, printing tests were conducted with different printing conditions.

The print tests were conducted on a Graber i3 model 3D printer, manufactured by GTMax3D®. This printer model includes a MK2B Dual Power PCB printing bed in contact with a thermistor type temperature sensor model NTC, which is located directly in contact with a 200 x 200 x 3 mm glass surface. The Graber i3 also contains a Hotend Allmetal GTMax 3D model extruder, which has a nozzle diameter of 0.4 mm. This printer model, according to the manufacturer, is capable of achieve a printing resolution of ±0.05 mm in X-Y and Z axis. The PLA filament utilized in the tests were manufactured by 3D Fila®. The print tests were controlled and supervised via a computer running the Repetier-Host® software. The connection between the computer and the 3D printer was made via a USB connection.

The slicing step of the print tests was conducted in the Slic3r® software, running as part of the Repetier-Host® software. In regard to the different printing conditions, three were established. A regular printing (RP) condition, in which a regular printing surface was obtained, and two irregular printing conditions, irregular printing 1 (IP1) and irregular

printing 2 (IP2), achieved by means of altering the value of the Z offset post processing parameter in the slicing step to 0.1 mm and -0.1 mm, respectively, in which the printing surfaces would show distinct defects.

In regard to the regular printing condition, Table 1 shows the post processing parameters adopted for the regular printing condition. For the regular printing condition post processing parameters that are not mentioned in Table 1, the default values provided by the Slic3r® software were adopted for printing with PLA and G-code RepRap flavor (Marlin/Sprinter). Forced cooling was not applied on the fabrication of the monolayer parts.

The digital model of the monolayer part was obtained by means of modelling in the SketchUp® software. Figure 1 shows the monolayer part model adopted for the printing tests after it has been sliced with regular printing condition post processing parameters. The sliced model presents two distinct infill patterns, the external and the internal infill patterns. The external infill pattern, commonly referred to as number of shells/contours/perimeters, consists of three contour lines, visually identified on Figure 1, that outline the four sides of the printed part. On the other hand, the internal infill pattern presents the fabrication of thirty raster lines, fabricated with a raster angle of 45º.

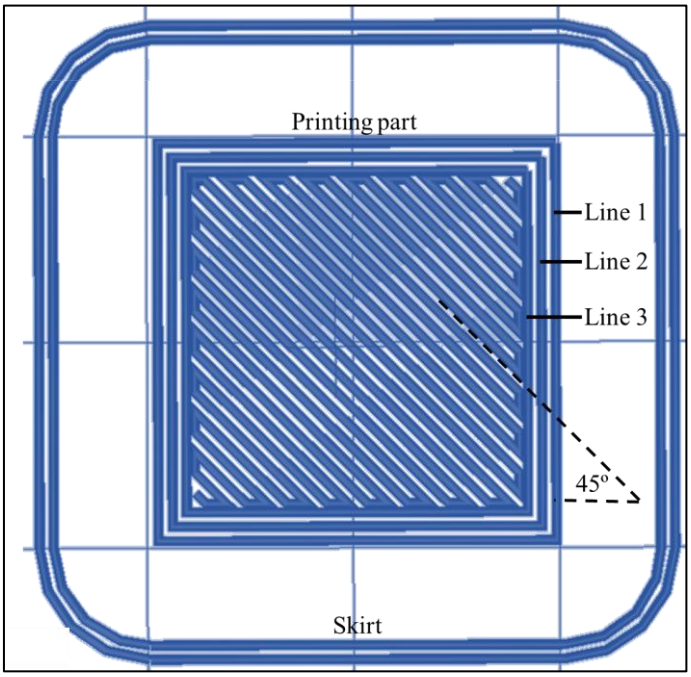

Figure 1. Workpiece model

Table 1 – Regular printing condition post processing parameters

Printing settings				
First layer height	**Seam position**	**Raster angle**	**Speed for non-print moves**	**Default extrusion width**
0.3 mm	Aligned	45°	50 mm/s	auto
First layer speed	**Top and Bottom external infill pattern**	**Skirt loops**	**Skirt distance from object**	**Skirt height**
20 mm/s	Rectlinear	2	4 mm	1 layer
Filament settings				
Filament diameter	**First layer extruder temperature**		**First layer bed temperature**	
1.75 mm	190 ºC		65 ºC	
Printer settings				
Nozzle diameter	**Z offset**		**Retraction length**	
0.4 mm	0 mm		0 mm	

3.2 Profilometry setup

The profilometry process was conducted with the aid of an experiment script produced especially for the printed monolayer parts, where a specific region was selected in order for the profilometry to be conducted, along with the dimensions of the selected region and the total dimensions of the part. As represented in Figure 2 for the regular printing

condition, the chosen profilometry region was established at the top section of the monolayer part, enclosing the three contour lines.

To carry out the measurements of roughness and topography of the printed parts, the Veeco non-contact optical profilometer, model Wyko NT100, was used. This device has a vertical resolution (z axis) of 1 angstrom and horizontal (x and y axis) of 1 to 2.5 micron in all magnifications and uses white light interferometry for high resolution three-dimensional surface measurements. The equipment is capable of measuring nanometric roughness and topographic measurements of up to 1 mm in height (z axis).

The Vertical Scanning Interferometry (VSI) measurement mode was applied, as the roughness and topography are in the micrometric order. A 2.5x magnification was used for all samples, considering a 0.5x multiplier lens and a 5x objective lens, generating images of 2.47 x 1.88 mm². From the images obtained in the process, it was possible to determine several measures of roughness.

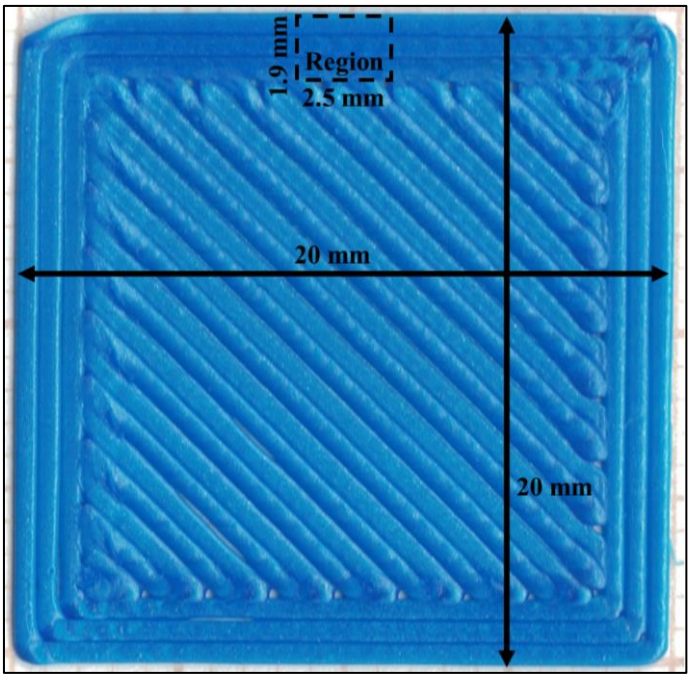

Figure 2. Experiment script for profilometry

3.3 Surface analysis

The surface analysis was conducted using the Vision version 4.20 software to open and interact with obtained profilometry images. Before doing any measurements, a mask was applied to all images to better the images' contrast and exclude outlying points. The masks were accomplished using the Histogram function on the Vision Mask Editor, where the histogram of the points' height was "cut" before the first and after the last height groups with a significant number of points, trying to avoid excluding valid points.

The following parameters were then measured: track width (considered as starting at the depression point where the profile starts an ascendant curve and ending at the analogous point on the other side of the wave); Ra, Rq and Rt of the profile, all measured in the same line used to measure the track width, and Sa, Sq and St of the whole track section present in the image.

4. RESULTS AND DISCUSSION

4.1 Visual inspection of profilometry images

By means of the optical profilometry and the Veeco software, it was possible to generate topographic images of the monolayer parts surfaces. With these images, measurements were made as shown in Figure 3. In Figure 3 (a), where the topography of the printed part in regular printing condition is represented, it can be seen that the measurements between valleys and the total measure of what would be the central peak, as well as the depth/height color scale, point to a regularity in the filament deposition, without any major flattening or lack of adhesion between the tracks.

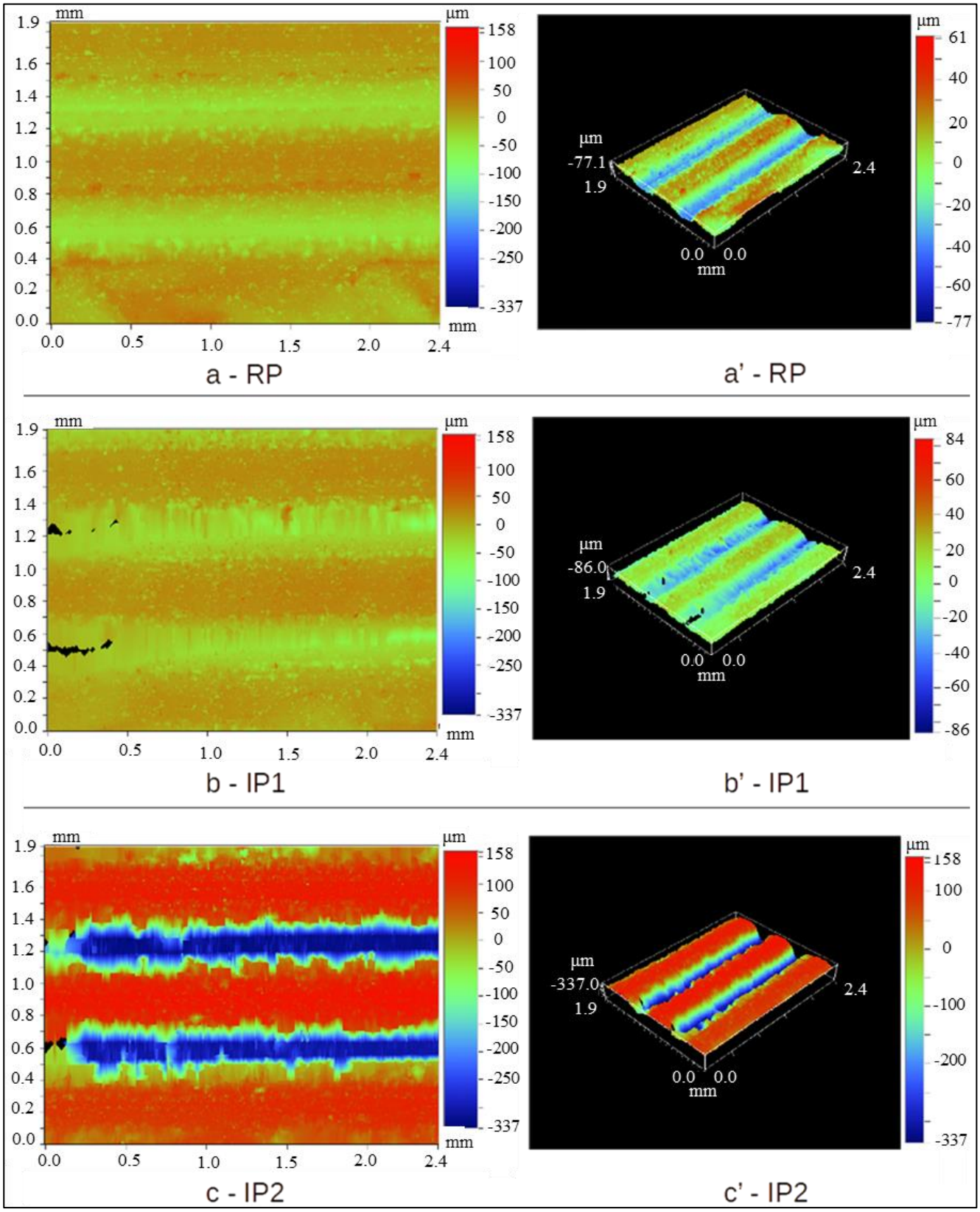

Figure 3. Optical profilometry images showing the 2D (a-c) and 3D (a'-c') surface topography.

In the case shown in Figure 3 (b) and (b'), where the topography of the printed part in the irregular printing 1 condition is represented, with the z axis closer to the printing bed, the image shows the flattening of the trails, resulting in overall

less prominent valleys and peaks and increased width in the peak regions, which are between the shades of green and orange.

What is evident in the images of the irregular printing 2 condition presented in Figure 3 (c) and (c'), in turn, is the opposite of what can be observed in the irregular printing 1 condition. The peaks are well marked in the shades of red, indicating higher altitudes in relation to the valleys, which are a shade of intense blue. It is also observed that the width of the central track is smaller in relation to the other printing conditions, which highlights the lack of adhesion between the tracks of the part. Such anomalies are compatible with the defective parameterization that was imposed on the part.

4.2 Surface roughness evaluation

Regarding the surface roughness evaluation of the printed monolayer parts, Table 2 shows the data from the area's surface roughness parameters, while Table 3 displays the data relative to the profile parameters.

Table 2 - Area surface roughness parameters data

Condition	Sa (µm)	Sq (µm)	St (µm)
IP1	13.2	15.5	87.13
RP	10.54	12.78	86.03
IP2	52.02	71.51	408.76

Table 3 - Profile parameters data

Condition	Track width (mm)	Ra (µm)	Rq (µm)	Rt (µm)
IP1	0.7515	19.3	21.91	71.28
RP	0.7128	17.82	20.12	64.76
IP2	0.5772	101.33	121.74	467.68

It can be seen that the RP has a slightly lower surface roughness than IP1and a dramatically lower roughness than IP2 for all the six studied parameters. The difference between the IP1 and RP conditions range from 1.3% for St to 25.3% for Sa, with an average difference of around 12.5%, suggesting that the experimental procedure indeed affected surface quality and that optical profilometry is a suitable technique to perceive the change. The small difference between St values could be due to either its nature, in the sense that a singular small, but deep, depression is enough to greatly influence the final result, or the limited number of samples tested. In the case of IP2, the discrepancy is such, in average 471% higher than RP, that even a quick visual inspection would be enough to reject the part in a production line, so, as much as the loss in quality can be quantified by the use of optical profilometer, the analysis would not really be needed for most applications.

In general, results for both types of roughness seem to agree with each other in terms of scale and ranking of the conditions. The considerable difference between the IP1 and the other printing conditions could be an effect of more frequent inter-track debonding caused by the somewhat looser filament deposition of this condition. Track widths seem consistent with what was to be expected i.e. for a constant material feed rate, and thus constant material volume, track width is inversely proportional to the extruder relative height to the bed.

5. CONCLUSION

The optical profilometry of the surfaces of the monolayer parts printed in PLA allowed the evaluation of superficial parameters and surface roughness caused by the selection of different post processing parameters in the slicing step of the FFF process. Through visual inspection of the profilometry images, it was possible to observe that the selection of certain post processing parameters influences the surface parameters of the obtained monolayer parts . It was also possible to observe, in this study, the same effects through the surface roughness evaluation of the parts.

Finally, it is concluded that with the use of optical profilometry to investigate the surface of monolayer parts obtained by the FFF process, it is possible to determine the occurrence of surface anomalies arising from an incorrect definition of post processing parameters during the slicing step, assisting the operator of the FFF process in decision making regard the characteristics of printing being adopted for a given process. Moreover, it is emphasized that the approach performed in this work is initial and additional studies are necessary in order to validate the proposed method under different slicing and printing conditions.

6. ACKNOWLEDGEMENTS

This work was supported by the São Paulo Research Foundation (FAPESP) (grants #2016/22038-8, #2019/22788-5 and #08/53641-5) and by the National Council for Scientific and Technological Development (CNPq) (grants #306435/2017-9)

7. REFERENCES

Adi, S. *et al. Scanning White-Light Interferometry as a Novel Technique to Quantify the Surface Roughness of Micron-Sized Particles for Inhalation*. Langmuir, [*s. l.*], v. 24, n. 19, p. 11307–11312, 2008.

Blunt, R.T. *White Light Interferometry - A production worthy technique for measuring surface roughness on semiconductor wafers*. *In*: , 2006. 2006 International Conference on Compound Semiconductor Manufacturing Technology. [*S. l.: s. n.*], 2006. p. 59–62.

Carmo, M.G.F. *et al. Study of the Defects and Geometric Anomalies on Monolayer Parts Obtained by Fused Deposition Modeling Process*. Proceedings, Online, v. 69, n. 1, p. 40, 2020.

Dhinakaran, V. *et al. A review on recent advancements in fused deposition modeling*. Materials Today: Proceedings, [*s. l.*], v. 27, p. 752–756, 2020.

Gantz, L. *et al. In vitro comparison of the surface roughness of polymethyl methacrylate and bis-acrylic resins for interim restorations before and after polishing*. The Journal of Prosthetic Dentistry, [*s. l.*], v. 125, n. 5, p. 833.e1-833.e10, 2021.

Khoshkhoo, A. *et al. Understanding and Engineering of Natural Surfaces with Additive Manufacturing*. *In*: , 2017, Austin, Texas. 28th International Solid Freeform Fabrication Symposium. Austin, Texas: [*s. n.*], 2017. p. 2350–2364.

Kocisko, M. *et al. Postprocess Options for Home 3D Printers*. Procedia Engineering, [*s. l.*], v. 196, n. June, p. 1065–1071, 2017.

Leksycki, K.; królczyk, J.B. *Comparative assessment of the surface topography for different optical profilometry techniques after dry turning of Ti6Al4V titanium alloy*. Measurement, [*s. l.*], v. 169, n. May 2020, p. 108378, 2021.

Liu, Z. *et al. A critical review of fused deposition modeling 3D printing technology in manufacturing polylactic acid parts*. The International Journal of Advanced Manufacturing Technology, [*s. l.*], v. 102, n. 9–12, p. 2877–2889, 2019.

Lopes, T.G. *et al. The first layer as a quality indicator of 3D printing process planning* (in Portuguese). *In*: , 2020, Bauru. Anais do XXVII Simpósio de Engenharia de Produção (SIMPEP). Bauru: [*s. n.*], 2020. p. 1–12.

Luo, D. *et al. Area scanning method for 3D surface profilometry based on an adaptive confocal microscope*. Optics and Lasers in Engineering, [*s. l.*], v. 124, n. February 2019, p. 105819, 2020.

Nieslony, P. *et al. Comparative assessment of the mechanical and electromagnetic surfaces of explosively clad Ti–steel plates after drilling process*. Precision Engineering, [*s. l.*], v. 47, p. 104–110, 2017.

Setti, D.; Kirsch, B.; Aurich, J.C. *Characterization of micro grinding tools using optical profilometry*. Optics and Lasers in Engineering, [*s. l.*], v. 121, n. December 2018, p. 150–155, 2019.

Spece, H. *et al. 3D printed porous PEEK created via fused filament fabrication for osteoconductive orthopaedic surfaces*. Journal of the Mechanical Behavior of Biomedical Materials, [*s. l.*], v. 109, p. 103850, 2020.

Tyagi, P. *et al. Reducing the roughness of internal surface of an additive manufacturing produced 316 steel component by chempolishing and electropolishing*. Additive Manufacturing, [*s. l.*], v. 25, n. October 2018, p. 32–38, 2019.

Volpato, N. *Additive Manufacturing: 3D printing technologies and applications* (in Portuguese). 1. ed. São Paulo: Blucher, 2017.

Wendt, C. *et al. Processing and Quality Evaluation of Additive Manufacturing Monolayer Specimens*. Advances in Materials Science and Engineering, [*s. l.*], v. 2016, p. 1–8, 2016.

Wu, H.; Yu, Z.; Wang, Y. *A New Approach for Online Monitoring of Additive Manufacturing Based on Acoustic Emission*. *In*: , 2016, Blacksburg. Volume 3: Joint MSEC-NAMRC Symposia. Blacksburg: American Society of Mechanical Engineers, 2016. p. 8.

Xu, J.; Ding, L.; Love, P.E.D. *Digital reproduction of historical building ornamental components: From 3D scanning to 3D printing*. Automation in Construction, [*s. l.*], v. 76, p. 85–96, 2017.

Yeh, C.C.; Chen, Y.F. *Critical success factors for adoption of 3D printing*. Technological Forecasting and Social Change, [*s. l.*], v. 132, n. January, p. 209–216, 2018.

Zhang, X. *et al. Correlation approach for quality assurance of additive manufactured parts based on optical metrology*. Journal of Manufacturing Processes, [*s. l.*], v. 53, n. May 2019, p. 310–317, 2020.

Zwier, M.P.; Wits, W.W. *Design for Additive Manufacturing: Automated Build Orientation Selection and Optimization*. Procedia CIRP, [*s. l.*], v. 55, p. 128–133, 2016.

8. RESPONSIBILITY NOTICE

The authors are the only responsible for the printed material included in this paper.